Kinetics of Cosurfactant−Surfactant−Silicate Phase Behavior. 1. Short-Chain Alcohols

Patrik Ågren,* Mika Lindén, and Jarl B. Rosenholm

Department of Physical Chemistry, Åbo Akademi University, Porthaninkatu 3-5, FIN-20500 Turku, Finland

Robert Schwarzenbacher, Manfred Kriechbaum, Heinz Amenitsch, and Peter Laggner

Institute of Biophysics and X-Ray Structure Research, Austrian Academy of Sciences, Steyrergasse 17/VI, A-8010 Graz, Austria

Juliette Blanchard and Ferdi Schüth

Department of Inorganic and Analytical Chemistry, Johann Wolfgang Goethe Universität, Marie Curie Strasse 11, D-60439 Frankfurt am Main, Germany

Received: December 9, 1998; In Final Form: April 19, 1999

The formation of hexagonal and lamellar surfactant−silicate mesophases at room temperature has been investigated by in situ synchrotron small angle X-ray scattering. Emphasis was given to the influence of butanol and hexanol on the surfactant−silicate phase behavior. The experimental setup included a continuous flow reactor allowing a resolution in time as high as 0.3 s. Depending on the reaction composition, one, two, or three coexisting phases were observed. The results are discussed in terms of time-dependent changes in the concentration of cosurfactant not incorporated into the composite aggregates. Although many of the observed effects are paralleled by well-known properties of aqueous surfactant solutions, important dissimilarities exist. Furthermore, the relative intensity of the high-order reflections are suggested to correspond to the degree of interaggregate condensation in the composite mesophase.

Introduction

The discovery[1,2] that surfactants can be used as templates for the synthesis of mesoporous oxides has attracted a lot of interest due to their potential applications in catalysis and biofiltration. A wide range of experimental conditions have been successfully applied in the synthesis of mesostructured silica varying with respect to temperature, nature of surfactant, surfactant concentration, pH, and silica source. Depending mainly upon the nature of surfactant used and on the silica/surfactant ratio, hexagonal, cubic, and lamellar structures have been synthesized.[3] The close resemblance between the mesophases observed for inorganic−surfactant composites and those observed in aqueous surfactant solutions suggests that the driving forces responsible for the mesophase formation are similar in both cases. However, composite mesophases are obtained at surfactant concentrations well below those needed to induce mesophase formation in aqueous surfactant solutions, which reflects the high degree of cooperativity of the process.

Polycharged silicate species will preferentially adsorb onto the micellar interface[4] since multivalent counterions usually interact much more strongly with charged interfaces than monovalent ions. The strong adsorption of silicate species onto the micellar interface may be expected to favor a transition to rodlike structures. Indeed, in a recent report[5] light scattering and rheology measurements indicated that negatively charged silica species (pH = 11.5−11.9) promote a sphere-to-rod transition of CTACl micelles. In situ EPR measurements[6] show a gradual transformation of the micellar spectrum into a characteristic rigid limit spectrum with time. The time required for long-range hexagonal order to occur is largely dependent on the silica source, pH, and temperature, with times ranging from some minutes to several hours reported in the literature.[7−9]

For dilute surfactant solutions where interaggregate interactions are of minor importance, a model has been developed to correlate the molecular geometry of the individual surfactant monomer to the observed aggregate structures.[9,10] The surfactant number, N_s, is defined as

$$N_s = v/la_o$$

where v is the volume of the hydrophobic tail, l is the effective length of the surfactant, and a_o is the effective area of the hydrophilic head group. For N_s values of 0.33, 0.5, and 1.0 spherical, rodlike, and lamellar geometries are expected to form. It is well-known that the aqueous phase behavior of surfactants is influenced by the presence of short-chain alcohols ($n_c \geq 4$).[12,13] These are accumulated in the palisade layer of the surfactant aggregates and are therefore referred to as cosurfactants. These cosurfactants will increase the effective value of N_s and therefore favor the formation of structures with a lower curvature. It has recently been shown that the low curvature, lamellar silicate−surfactant phase may be induced by the addition of hexanol.[14]

We report here in situ small angle synchrotron X-ray scattering results on the mesostructure formation in a room temperature synthesis of silica−surfactant composites with emphasis on the influence of cosurfactant concentration and chain length. The high intensity of the synchrotron beam and the experimental setup including a continuous-flow reactor allowed a resolution in time as high as 0.3 s, and therefore detailed information about the initial stages of cosurfactant−surfactant−silicate mesophase formation was obtained.

10.1021/jp984684x CCC: $18.00
Published on Web 06/06/1999

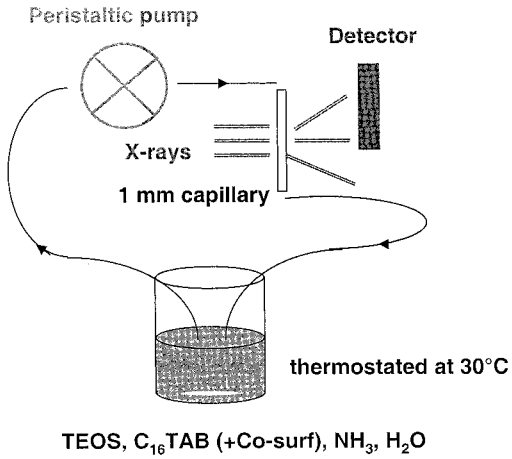

Figure 1. Schematic description of the batch reactor setup. See text for details.

Experimental Details

Materials. The following chemicals were used in the synthesis: Ammonia (25%) and butanol (99.5%) (BuOH) were supplied by Merck. Hexanol (98%) (HeOH), hexadecyltrimethylammonium bromide (CTAB), and tetraethylorthosilicate (TEOS) were obtained from Aldrich. All chemicals were used as received. The water was purified by distillation and deionization.

Synthesis. Typically, the synthesis was prepared as described below. An aliquot of 2.4 g of CTAB was dissolved in 120 g of water. When the CTAB had dissolved, HeOH or BuOH and 10 mL of ammonia were added and the solution was stirred until a clear solution was achieved. Finally, 9.4 g of TEOS was carefully added to the mixture in order to avoid initial mixing with the aqueous solution. Before addition of TEOS the pH was $pH_{ini} = 11.8$ and after addition of TEOS it was $pH_{fin} = 10.7$.

Batch Reactor. The batch reactor is schematically presented in Figure 1. The setup consists of a beaker containing the synthesis mixture, a peristaltic pump, tubing, and a quartz capillary. With this setup the synthesis mixture flowing through the capillary was recycled by pumping it back to the batch reactor. The reaction was started by initiating the mixing of the two-phase solution and at the same time the pumping was started. The two-phase synthesis solution was pumped through a 1 mm o.d. quartz capillary at a pumping rate of 25 mL/min. Both the batch reactor and the capillary were thermostated to 30 °C. With the in situ setup used in the present investigation the reaction may be studied without changing the ratio between the different components in the synthesis mixture. Furthermore, the setup was used instead of a static one in order to stabilize the TEOS−water emulsion and to maintain the precipitated mesophase homogenously dispersed in the solution. The reaction time is always the same in the tubing and quartz capillary as in the batch reactor and therefore the result presents a simple means for detailed kinetic studies.

X-ray Analysis. The quartz capillary was centered in the X-ray beam. The SAXS measurements were performed in a resolution range from 80 to 19 Å, with an exposure time down to 0.3 s, at the Austrian high-flux SAXS beamline of the 2 GeV electron storage ring ELETTRA, Trieste, Italy.[15] The radiation wavelength was 1.542 Å. The data were collected on a linear position-sensitive Gabriel detector, which enabled simultaneous detection of the whole angle range.

Results

TEOS/H_2O/CTAB/NH_3. The formation of hexagonally ordered material as a function of time is shown in Figure 2a,b. Mesophase formation was completed within the first 5 min after mixing of the reactants. One can observe a low angle Bragg reflection in the diffractogram after 80 ± 10 s. Two other reflections that could be indexed assuming a hexagonal unit cell appeared shortly after. These results parallel those recently published concerning the development of the hexagonal mesophase in this system studied by in situ XRD using a tubular reactor setup.[7] Two interesting features were evident. The reflections shifted to higher angles, i.e., lower *d* spacings with time, being 4.67 and 4.48 nm at 100 and 500 s, respectively. Furthermore, the intensity of the 200 reflection was initially higher than that of the 110 reflection, while the opposite was observed at longer reaction times. This also holds true for all observed hexagonal mesophases for the alcohol/CTAB systems described below. The intensity of all reflections increased with time, indicative of an increased ordering and a higher solid content of the solution. No intermediate phases were observed. Although it is principally possible using SAXS to distinguish between spherical and rodlike micelles from the diffuse scattering curve,[16] compromises had to be made in the experimental design to obtain information from both the diffuse part and the Bragg region of the scattering curve. This resulted in loss of resolution in the diffuse part, and therefore a distinction between spherical and rodlike micelles was not possible in our case. However, micelles were detected both before and after the addition of TEOS in the low-angle region of the scattering curve. The intensity of the diffuse scattering indicative of micelles decreased gradually as the intensity of the Bragg peaks increased.

Influence of HeOH. Addition of HeOH (0.3 g) led to a much more complex phase behavior. Again, a small-angle reflection appeared after approximately 80 s after mixing. Immediately after its appearance, this peak "wiggled" to larger *d* values. Two high-order reflections, indicated that this structure can be indexed assuming a two-dimensional hexagonal symmetry. The evolution of the reflections as a function of time is shown in Figure 3a,b. In this case, a "swollen" hexagonal (H′) phase with an initial *d* spacing of 5.00 nm was observed. A second low-angle reflection (H″) appeared about 150 s after mixing with a *d* spacing of 4.78 nm together with two high-order reflections that could also be indexed assuming a hexagonal symmetry. As in the absence of HeOH, the 200 reflection was initially higher than that of the 110 reflection but turned to the contrary at longer reaction times. This feature is not as evident in the case of the H″ phase, because the higher-order reflection intensities are not as high. The *d* spacings of both phases decreased with reaction time to reach 4.85 nm (H′) and 4.60 nm (H″) at 500 s, respectively.

Increasing the added amount of HeOH to 0.5 g led to the initial formation of a coexisting "swollen" hexagonal (H′) together with a lamellar (L′) phase, as shown in Figure 4. The corresponding *d* spacings 100 s after mixing were 5.36 nm (H′) and 4.67 nm (L′), respectively. A second hexagonal (H″) phase with an initial *d* spacing of 4.82 nm appeared about 150 s after mixing. All phases contracted upon increasing reaction time to reach a *d* spacing 100 (001 for the lamellar phase) of 5.00 nm (H′), 3.68 nm (L′), and 4.54 nm (H″), respectively, at a reaction time of 500 s. Note that the 002 reflection of the lamellar phase falls out of the detector range after about 200 s because of phase

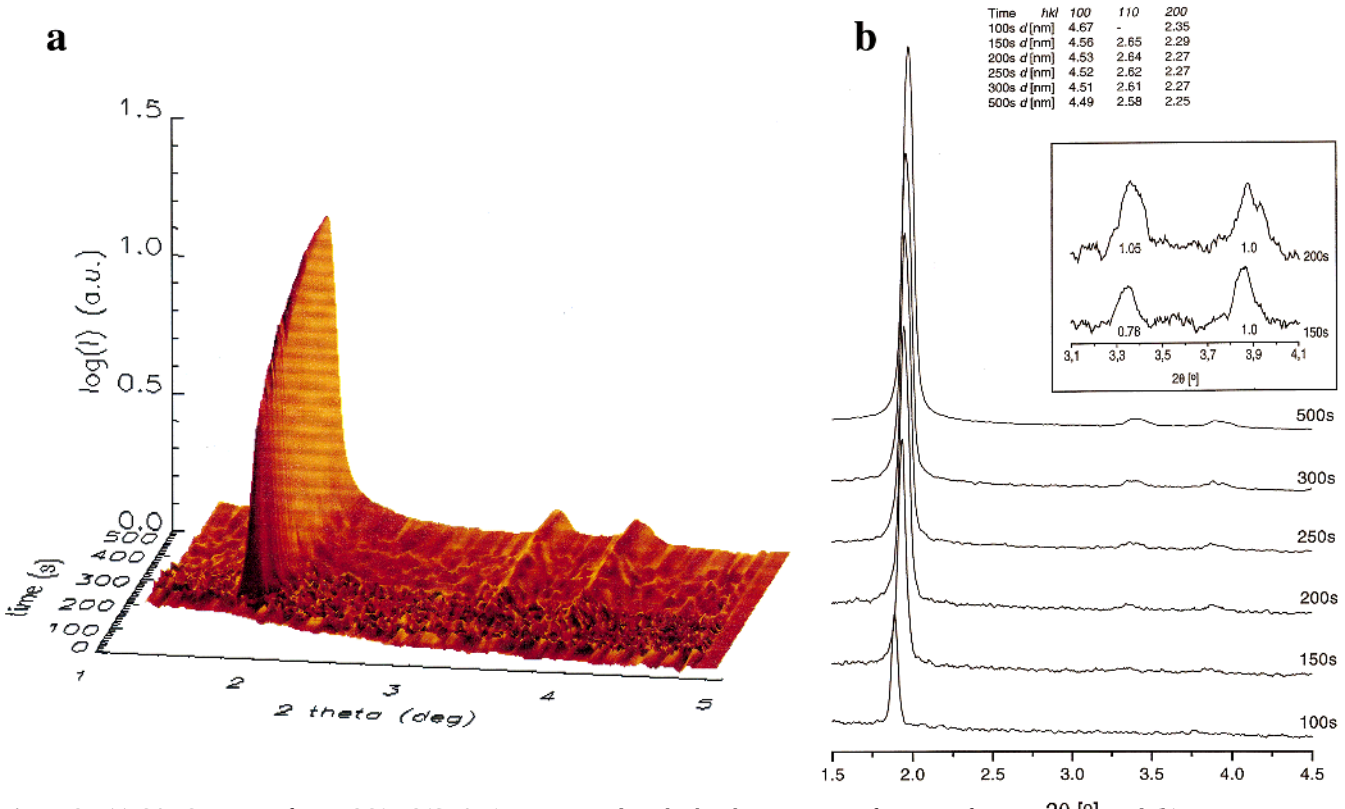

Figure 2. (a) SAXS patterns for TEOS/H_2O/CTAB/NH_3 prepared in the batch reactor as a function of reaction time and (b) XRD patterns at various times after mixing of reactants. Inset: magnification of the 110 and 200 reflections (numbers indicate the intensity ratio of the 110/200 reflections).

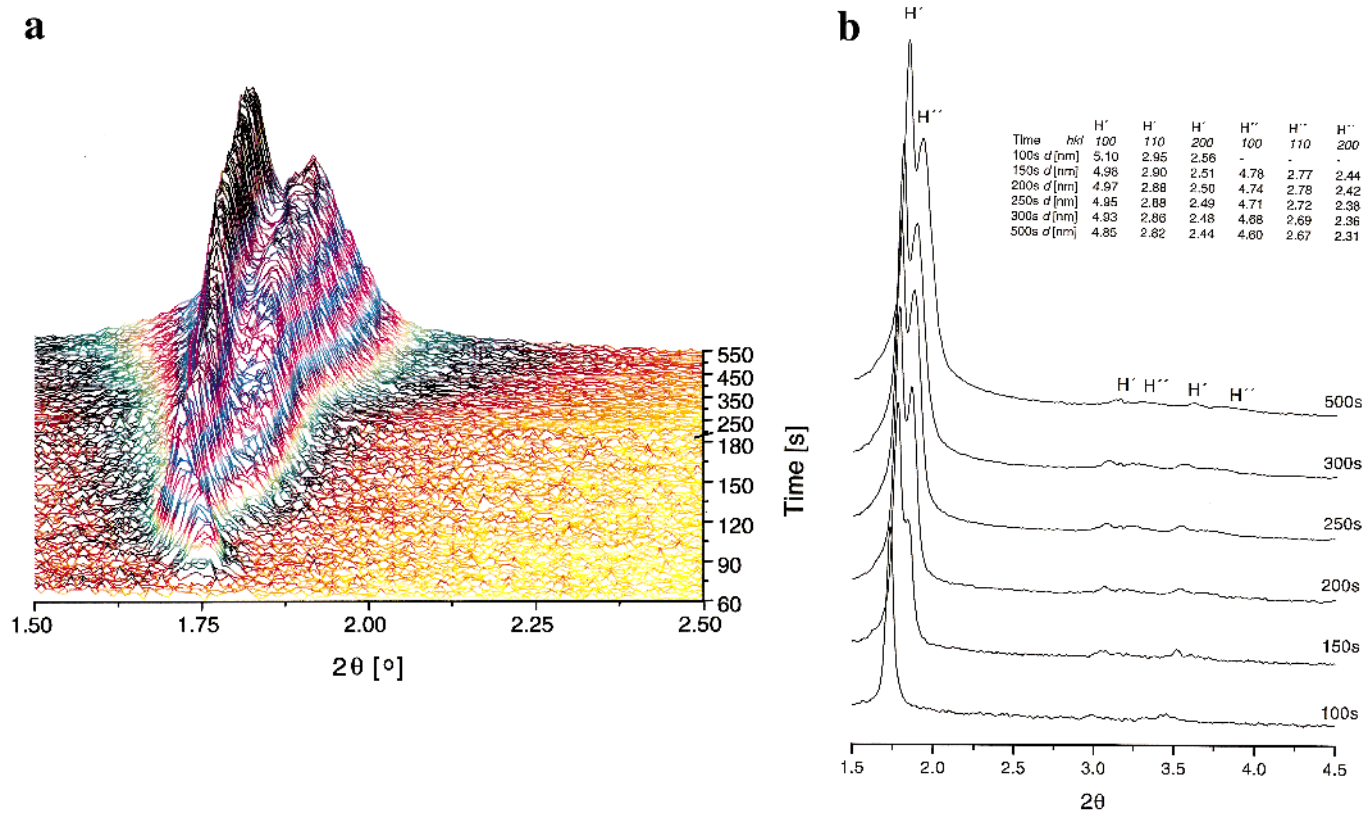

Figure 3. XRD patterns with HeOH (0.3 g) as cosurfactant prepared in the batch reactor (a) as a function of reaction time (note the discontinuity in the time axis after 185 s of mixing) and (b) at various times after mixing of reactants. H′ and H″ indicate the hexagonal phases.

contraction. However an intermediate increase to slightly higher *d* spacings was again observed for the H′ phase.

Addition of 0.6 g of HeOH led to a purely lamellar mesophase, as shown in Figure 5, with no other coexisting

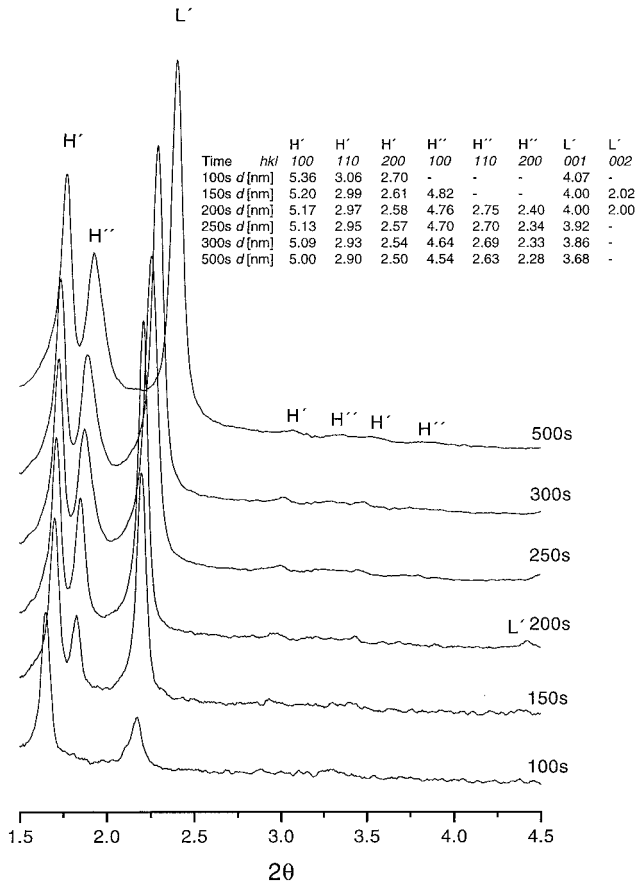

Time	hkl	H´ 100	H´ 110	H´ 200	H´´ 100	H´´ 110	H´´ 200	L´ 001	L´ 002
100s	*d* [nm]	5.36	3.06	2.70	-	-	-	4.07	-
150s	*d* [nm]	5.20	2.99	2.61	4.82	-	-	4.00	2.02
200s	*d* [nm]	5.17	2.97	2.58	4.76	2.75	2.40	4.00	2.00
250s	*d* [nm]	5.13	2.95	2.57	4.70	2.70	2.34	3.92	-
300s	*d* [nm]	5.09	2.93	2.54	4.64	2.69	2.33	3.86	-
500s	*d* [nm]	5.00	2.90	2.50	4.54	2.63	2.28	3.68	-

Figure 4. XRD patterns with HeOH (0.5 g) as cosurfactant prepared in the batch reactor at various times after mixing of reactants. H′ and H″ indicate the hexagonal phases, and L′ indicates the lamellar phase.

phases. The phase was formed about 80 s after mixing, and the *d* spacing for the 001 reflection was 4.09 nm after 100 s of mixing. The phase contracted upon increasing reaction time to reach a *d* spacing of 3.71 nm at a reaction time of 500 s. Note that the 002 reflection falls out of the detector range about 250 s after mixing. No intermediate oscillation in *d* spacing was observed. Generally, an increase in the HeOH content leads to the formation of structures with lower curvature and higher extent of swelling of the "swollen" hexagonal phase.

Influence of BuOH. Similar experiments were performed using BuOH as the cosurfactant. When 0.6 g of BuOH were added to the synthesis mixture, a small-angle reflection appeared about 80 s after initiating mixing (results not shown). Two high-order reflections appeared shortly after, which could be indexed by assuming a hexagonal symmetry. The *d* spacing after 100 s of mixing was slightly higher, 4.77 nm (H′), than in the absence of BuOH. Again, the H′ phase showed an intermediate increase to slightly higher *d* spacings shortly after the formation of the mesophase. After about 200 s of mixing another coexisting hexagonal (H″) phase was formed with an initial 100 *d* spacing of 4.56 nm, which is almost the same value as observed in the absence of BuOH. Both phases contracted with reaction time, reaching 4.58 nm (H′) and 4.47 nm (H″), respectively, after 400 s of mixing.

Increasing the added amount of BuOH to 1.5 g led to a hexagonal structure with a slightly higher *d* spacing than the previous experiment. The *d* spacing was 4.82 nm (H′) after 100 s of mixing. Around the same time the 200 reflection appeared, followed by the 110 reflection (results not shown). Again, the *d* spacing of this phase increased slightly at the initial stages of structure formation. A second hexagonal (H″) phase with a *d* spacing of 4.58 nm could be observed after about 150 s of

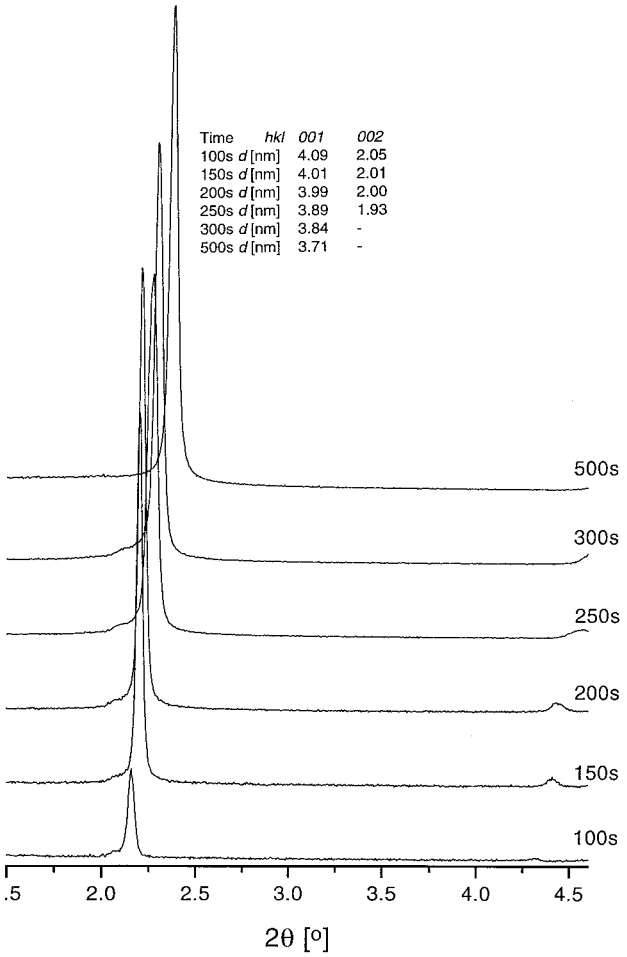

Time	hkl	001	002
100s	*d* [nm]	4.09	2.05
150s	*d* [nm]	4.01	2.01
200s	*d* [nm]	3.99	2.00
250s	*d* [nm]	3.89	1.93
300s	*d* [nm]	3.84	-
500s	*d* [nm]	3.71	-

Figure 5. XRD patterns with HeOH (0.6 g) as cosurfactant prepared in the batch reactor at various times after mixing of reactants.

mixing. The *d* spacings decreased with time to reach 4.68 nm (H′) and 4.53 nm (H″), respectively, after 300 s of mixing.

Adding 3 g of BuOH led to the same phase behavior as observed for 0.5 g of HeOH, with two coexisting hexagonal (H′ and H″) phases together with a lamellar phase (L′). The initially formed phase was the lamellar (L′) followed by the hexagonal (H′) phase, and finally the coexisting hexagonal (H″) phase was formed. All phases contracted upon increasing reaction time (results not shown).

However, when increasing the amount of added BuOH to 5 g, two coexisting lamellar structures, denoted L′ and L″, respectively, were formed with different kinetics of formation. The L′ phase, with a *d* spacing of 3.94 nm, could be observed already after 100 s of mixing. After about 150 s of mixing the L″ phase with a *d* spacing of 3.98 nm was formed. The structure first contracts, then expands, and finally remains almost constant in size. No subsequent contraction could be observed because the measurement time in this case was only 200 s. Generally, an increase in the BuOH content leads to the formation of structures with lower curvature and higher extent of swelling of the initially formed hexagonal phase.

Discussion

Regardless of the composition of the reaction mixtures studied, several common time-dependent features were observed: (i) the onset of mesoscopic order was observed approximately 80 s after mixing of the reactants, (ii) a contraction of the mesophases occurred with increasing reaction time, (iii) the intensity of all reflections increased with reaction time (<500 s), and (iv) the relative intensity of the 110 reflection

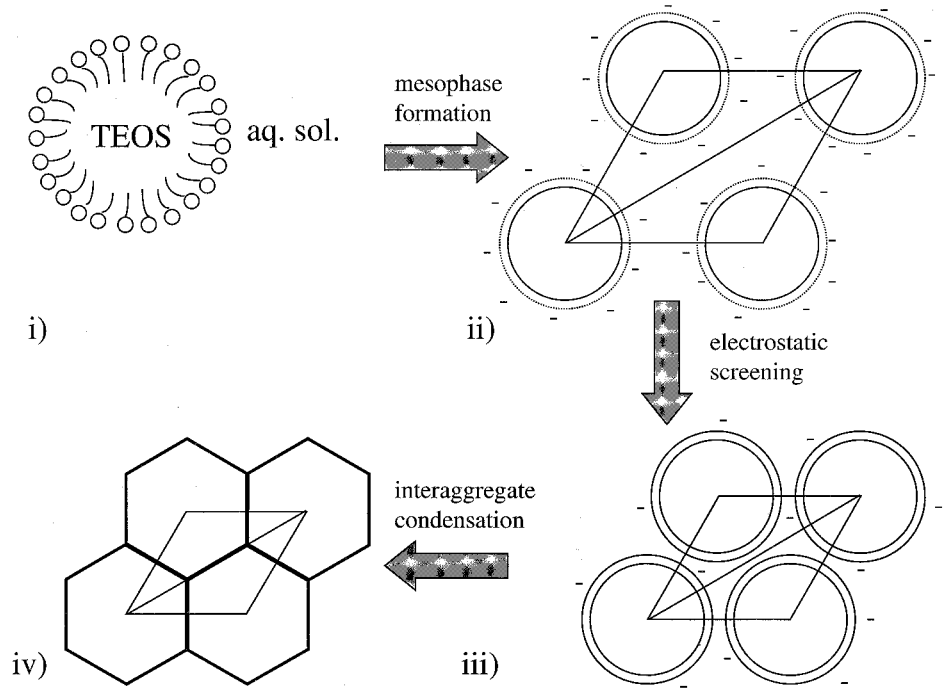

Figure 6. Schematic representation of the decrease in the size of the unit cell of the hexagonal mesophase with time: (i) CTAB emulsifying TEOS in the aqueous solution; (ii) cooperative mesophase formation with partially condensed and highly ionized silicate around the surfactant aggregates; (iii) electrostatic screening reducing the repulsive forces between the composite aggregates; (iv) inter(and intra)aggregate condensation maximizing the inorganic−inorganic contact between the composite aggregates.

of the hexagonal phase compared to that of the 200 reflection increased as a function of reaction time.

In the reaction, CTAB helps to emulsify the TEOS and the increased surface to volume ratio will increase the rate of hydrolysis, which is a prerequisite for the fast mesophase formation observed in this study. The emulsion formed is very unstable but is stabilized by the introduced mixing energy. Negatively charged hydrolysis products will be electrostatically adsorbed to the positively charged surfactant aggregates, inducing a sphere-to-rod transition of the composite aggregates[5] paralleled by cooperative mesophase formation.[9]

Contraction of the formed structures as a function of reaction time has been observed earlier for M41S type materials using ex situ experiments.[6,17] However, already the initially formed mesophase structures are fairly close-packed compared to corresponding CTAB mesophases with a high water content, for which a *d* spacing exceeding 170 Å has been observed due to the presence of free water between the hexagonally packed surfactant rods.[13]

The increase in intensity ratio of the 110/200 reflections observed here for silica has also been observed for hexagonally ordered zirconia[18] and explained as follows:[18] Due to the highly flexible nature of a composite mesostructure at a low degree of condensation the aggregates will behave similar to normal surfactant aggregates and the hexagonal mesophase consists of close-packed rodlike composite aggregates with a circular cross-section. However, when the degree of condensation increases, the geometry will gradually change due to interaggregate condensation to maximize inorganic−inorganic contact, as schematically shown in Figure 6. This structural change will increase the amount of inorganics (good scatterers) along the 110 axis, while no strong change in scatterer density along the 100 (or 200) axis occurs. This effect would account for the observed increase in the intensity of the 110 reflection with time. Although the formation of hexagonally shaped pores would result in an energetically favorable constant wall thickness, we do not have any evidence at the time proving that this is the case. However, the intensity of the 110 reflection is not dependent on the geometry of the pore but on the total density of scatterers along the 110 axis. The observation that the increase in the intensity of the 110 reflection is paralleled by a decrease in the *d* spacing supports the idea that the contraction is caused by a decrease in interaggregate electrostatic repulsion upon condensation.

Influence of Cosurfactants. The kinetics of mesophase formation was not affected by the addition of either BuOH or HeOH. This suggests that the addition of small amounts of alcohol does not have a large influence on the speciation of the silicate. However, medium chain-length alcohols as cosurfactants are known to decrease the curvature of micelles and surfactant aggregates, promoting transitions from spherical to rodlike micelles and hexagonal to lamellar mesophases, etc.[13,19] It has also been reported in the literature[19−24] that in the system CTAB−alcohol−water, the alcohol ($n_c \geq 4$) will solubilize not only in the palisade layer but also in the interior of the micelle, thus swelling the micelle. The degree of swelling is proportional to the amount of added alcohol as well as on the alcohol chain length, since the micelle/bulk partition coefficient is about 10 times lower for BuOH than for HeOH due to its more hydrophilic character.[20] HeOH will also have a more pronounced influence on the value of the packing parameter due to its larger molecular size compared to BuOH. If increasing amounts of alcohol are added to aqueous solutions quite rich in CTAB, mesophases are formed in the order hexagonal (1ϕ), hexagonal−lamellar (2ϕ), lamellar (1ϕ); i.e., structures with lower curvature are formed when more alcohol is added. The reported hexagonal−lamellar (2ϕ) phases are highly viscous and do not phase separate and therefore Bragg reflections from both the hexagonal and lamellar structures are observed.[12,25]

We observed the same influence of the addition of alcohol on the composite mesophase formation: (i) the hexagonal composite structures showed a general feature of swelling, i.e., increased *d* spacings, upon addition of BuOH or HeOH; (ii) the extent of swelling increased with the concentration and chain length of the cosurfactant; (iii) a transition from the high-curvature hexagonal phase to a lamellar phase via a two-phase,

hexagonal−lamellar, region was observed with increasing alcohol content. It is known that one can swell the micelles and even the MCM-41 structures with auxiliary organics.[2] The decrease in the effective dielectric constant of water due to the addition of alcohol is expected to be small at the low alcohol concentrations used in this study and could not account for the observed increase in *d* spacing with increasing alcohol content of the solution. Further support for this claim is given by the fact that the subsequently formed hexagonal phase H″ has a very similar *d* spacing to that of the H′ phase formed in the absence of cosurfactant. Therefore, it is most likely even in our case that the cosurfactant is solubilized in both the palisade layer and the interior of the composite aggregates.

The cosurfactant/CTAB ratio might change during the synthesis, depending on the partition between the bulk, free micelles, and composite aggregates. If the affinity of the cosurfactant for the composite aggregates is higher than the affinity for the free surfactant micelles, the effective concentration of cosurfactant not taking part in the composite mesophase formation will decrease during the reaction. This effect would explain the observed feature that the new phases observed at longer reaction times, H″ and L″, had lower *d* spacings compared to H′ and L′, respectively, since less swollen micellar structures will then act as templates for the subsequently formed phases. It has been reported that the *d* spacing of the lamellar phase in the CTAB−alcohol−water system changes with the cosurfactant/CTAB ratio.[13] In order to achieve a purely lamellar or swollen hexagonal composite mesostructure, one has to have an optimal cosurfactant/CTAB ratio during the whole synthesis.

The oscillation of the *d* spacings to higher values at initial stages of the synthesis might be explained by a redistribution of cosurfactants and CTAB between the micelles and the composite aggregates. It is important to remember that the composite systems reported on here are in a nonequilibrium state during the measurements due to the continuous changes in the chemical state of the reactants caused by hydrolysis and condensation of TEOS and the adsorption of ionized hydrolysis products to the surfactant aggregates. This is opposite to aqueous surfactant solutions that are normally investigated at equilibrium. Therefore, it is highly probable that the surfactant properties of the CTAB−silicate complexes are time-dependent. For instance, it is well known that by changing the salinity one can alter the amount of auxiliary organics that ionic micelles can solubilize.[26] It has also been reported that the extent of micelle swelling with alcohols can be further increased with addition of salt.[20] The ionic strength of the reactant solution will increase rapidly if highly charged silicate oligomers are formed. These time-dependent changes could surely account for the observed initial "wiggling" to higher *d* spacings at short reaction times in the presence of alcohol and also the swelling of the aggregates with increasing alcohol content of the solution. Furthermore, a change in the surfactant properties might explain the appearance of the L′ after the H′ in the system containing 0.5 g of HeOH. The lamellar phase requires more cosurfactant than the hexagonal phase to form. It seems that the surfactant properties change within 10 s to incorporate the required amount of cosurfactant to build a lamellar phase. On the other hand, since the H′/L′ ratio changes during the synthesis, the amount of the L′ phase might be so low when H′ appears that it is not yet detectable. Hence, in less than 10 s the amount of L′ increases to a detectable amount.

Summary

The influence of BuOH and HeOH on the mesoscopic ordering of silicate−CTAB mesophases has been studied by synchrotron SAXS equipped with a continuous flow reactor. The addition of either alcohol favors lower curvature structures, the effect of HeOH being much more pronounced compared to BuOH. Depending on the reaction composition, one, two, or three coexisting phases were observed. The observed effects can be explained on the basis of the micelle/bulk partition coefficients of the two alcohols and assuming a higher affinity of the alcohols for the composite aggregates compared to the micelles. Future experiments will focus on using short-chain amines as cosurfactants.

Acknowledgment. The authors wish to thank Dr. Sune Backlund and MSc Stefan Karlsson for fruitful discussions. The Ministry of Education (Finland) (GSMR), MATRA project, and EU project ERB-FMRX CT96-0084 are acknowledged for financial support.

References and Notes

(1) Kresge, C.T.; Leonowicz, M.E.; Roth, W.J.; Vartuli, J.C. *Nature*. **1992**, *359*, 710.

(2) Beck, J.S.; Vartuli, J.C.; Roth, W.J.; Leonowicz, M.E.; Kresge, C.T.; Schmitt, K.D.; Chu, C.T.-W.; Olson, D.H.; Sheppard, E.W.; McCullen, S.B.; Higgins, J.B.; Schlenker, J.L. *J. Am. Chem. Soc.* **1992**, *114*, 10834.

(3) Vartuli, J.C.; Schmitt, K.D.; Kresge, C.T.; Roth, W.J.; Leonewicz. M.E.; Mullen, S.B.; Hellring, S.D.; Beck, J.S.; Schlenker, J.L.; Olson, D.H.; Sheppard, E.W. *Chem. Mater*. **1994**, *6*, 2317.

(4) Firouzi, A.; Kumar, D.; Bull, L.M.; Besier, T.; Sieger, P.; Huo, Q.; Walker, S.A.; Zasadzinski, J.A.; Glinka, C.; Nicol, J.; Margolese, D.; Stucky, G.D.; Chmelka, B.F. *Science* **1995**, *267*, 1138.

(5) Lee, Y.S.; Surjadi, D.; Rathman, J.F. *Langmuir* **1996**, *12*, 6202.

(6) Zhang, J.; Luz, Z.; Goldfarb, D. *J. Phys. Chem.* **1997**, *101*, 7087.

(7) Lindén, M.; Schunk, S.; Schüth, F. *Angew. Chem., Int. Ed.* **1998**, *37*, 821.

(8) O'Brien, S.; Francis, R. J.; Price, S. J.; O'Hare, D.; Clark, S. M.; Okazaki, N.; Kuroda, K. *J. Chem. Soc., Chem. Commun.* **1995**, 2423.

(9) Monnier, A.; Schüth, F.; Huo, Q.; Kumar, D.; Margolese, D.; Maxwell, R. S.; Stucky, G. D.; Krishnamurty, M.; Petroff, P.; Firouzi, A.; Janicke M.; Chmelka, B. F. *Science* **1993**, *261*, 1299.

(10) Israelachvili, J.N.; Mitchell, D.J.; Ninham, B.W. *J. Chem. Soc., Faraday Trans. 2* **1976**, *72*, 1525.

(11) Israelachvili, J.N.; Mitchell, D.J.; Ninham, B.W. *Biochim. Biophys. Acta* **1977**, *470*, 185.

(12) Ekwall, P.; Mandell, L.; Fontell, K. *J. Colloid Interface Sci.* **1969**, *29*, 639.

(13) Fontell, K.; Khan, A.; Lindström, B.; Maciejawska, D.; Puang-Ngern, S. *Colloid Polym. Sci.* **1991**, *269*, 727.

(14) Firouzi, A.; Schaefer, D.J.; Tolbert, S.H.; Stucky, G.D.; Chmelka, B.F. *J. Am. Chem. Soc.* **1997**, *119*, 9466.

(15) Amenitsch, H.; Bernstorff, S.; Laggner, P. *Rev. Sci. Instrum.* **1995**, *66*, 1624.

(16) Glatter, O. In *Modern Aspects of Small-Angle Scattering*; Brumberger, H., Eds.; Kluwer Academic Publishers: Dordecht, The Netherlands, 1995.

(17) Regev, O. *Langmuir* **1996**, *12*, 4940.

(18) Lindén, M.; Schacht, S.; Schunk, S.; Schüth, F. Manuscript in preparation.

(19) Vikholm, I.; Douhéret, G.; Backlund, S.; Høiland, H. *J. Colloid Interface Sci.* **1987**, *116*, 582.

(20) Zana, R.; Yiv, S.; Strazielle, C.; Lianos, P. *J. Colloid Interface Sci.* **1981**, *80*, 208.

(21) Candau, S.; Zana, R. *J. Colloid Interface Sci.* **1981**, *84*, 206.

(22) Zana, R.; Picot, C.; Duplessix, R. *J. Colloid Interface Sci.* **1983**, *93*, 43.

(23) Hirsch, E.; Canau, S.; Zana, R. *J. Colloid Interface Sci.* **1984**, *97*, 318.

(24) Lianos, P.; Zana, R. *J. Colloid Interface Sci.* **1984**, *101*, 587.

(25) Mandell, L.; Ekwall, P. *Acta Polytech. Scand.* **1968**, *74*, 1.

(26) Shinoda, K.; Friberg, S. *Emulsions and Solubilization*; John Wiley & Sons, Inc.: New York, 1986.